Effect of Humidity on Copper Separation During High-Temperature Atmospheric Oxidation of Si-Containing Carbon Steels With 0.3 and 0.55 Copper Contents

David Landi[1], Emmanuel De Moor[2]

[1]Advanced Steel Processing and Products Research Center
Colorado School of Mines
1500 Illinois Street, Golden, Colorado, USA, 80401
Phone: 303-273-3624
Email: landi@mines.edu

[2] Advanced Steel Processing and Products Research Center Colorado School of Mines
1500 Illinois Street, Golden, Colorado, USA, 80401
Phone: 303-273-3624
Email: edemoor@mines.edu

ABSTRACT

Cu hot shortness due to increasing residual content within scrap can present challenges. Changes in atmospheric humidity during high temperature oxidation have been theorized to alter the steel/scale interface and promote scale adhesion, enhancing subsequent Cu penetration, but no direct correlation has been observed. In this work, 0.1C-0.25Si steels with 0.3Cu and 0.55Cu contents were studied using thermogravimetric analysis (TGA) at 1150 ℃ for 10 minutes in -28 ℃ and 35 ℃ dew point (DP) simulated air. Metallographic analysis to evaluate Cu separation during oxidation was conducted, and the steel/scale interfaces were observed using LOM. The oxidation behavior for both alloys in the -28 ℃ atmosphere was similar. The 35 ℃ DP atmosphere increased the parabolic oxidation rate of both alloys, and induced the linear-parabolic oxidation transition at a shorter time for the 0.3Cu alloy. No Cu separation was observed in the 0.3Cu alloy in the dry atmosphere, but discrete Cu particles and large Cu pools were found in the 0.55Cu alloy. The interfacial oxide became more adherent and contained a fine-scale oxide, likely fayalite, for both alloys in the wet atmosphere. Cu separation was observed for both alloys, manifesting as finely dispersed Cu particles along the interface and occluded into the adherent scale. These results suggest that increased humidity in ambient air can alter Cu separation at 1150 ℃ compared to dry air via promoting occlusion due to Si-rich interfacial oxide formation which disrupts the agglomeration of liquid Cu at the steel/scale interface, potentially accommodating greater residual Cu content in Si-containing steels.

Keywords: Copper Hot Shortness, Thermogravimetric Analysis (TGA), Scale Formation, Reheating, Dew Point, Occlusion

INTRODUCTION

During the casting, reheating, or hot charging stages of steel processing, significant oxide or “scale” forms. The oxidation of steel containing Cu can lead to the phenomenon of Cu hot shortness, where solute Cu locally enriches at the steel/scale interface and phase separates into a liquid at sufficient concentrations[1–4]. This liquid Cu-rich phase can penetrate along austenite grain boundaries and cause surface cracks ranging from cosmetic to significant mechanical defects which can result in processing challenges during subsequent rolling operations[5, 6]. Cu hot shortness susceptibility and appropriate mitigation strategies have become an area of increasing interest as scrap-based steelmaking practices become more prevalent and gradually enrich noble residual contaminants, such as Cu and Sn, in the scrap stream[7-10]. Industrial decarbonization trends have popularized electric arc furnace (EAF) scrap steelmaking routes to reduce emissions, making scrap-related steelmaking challenges a major obstacle to overcome for the adoption of “green steel” practices[11–13].

Several factors contribute to the Cu hot shortness behavior of an alloy, primarily alloy composition, processing temperature, oxidizing time and atmosphere. The effects of varying oxidizing time and combustion gas atmosphere (reheat, hydrogen) on Cu hot shortness susceptibility in plain carbon steels have been studied extensively, but the effects of humidity variations in

atmospheric (ambient air) conditions on the Cu hot shortness behavior are less well understood[14–18]. Most work has focused on the effects of varying H_2O resulting from varying fuel/air ratios in combustion furnaces, but less work has been done with high O_2-high H_2O atmospheres[19–23]. Research by Kim and Lee suggest that increased water vapor content can promote a more planar steel/scale interface during oxidation, promoting Cu-rich liquid contact with the base metal[24]. This is theorized to exacerbate Cu hot shortness, as a rougher interface may promote occlusion of the liquid into the scale, minimizing penetration along grain boundaries[25, 26]. In this work, the effects of varying atmospheric humidity on the oxidation behavior and subsequent Cu hot shortness response of 0.1C steels containing 0.25 wt pct Si with 0.3 and 0.55 wt pct Cu additions were investigated. Testing was conducted at 1150 ℃ for 10 minutes in -28℃ and 35℃ dew point (DP) simulated air to simulate conditions during reheating or tunnel furnace equalization and holding.

EXPERIMENTAL PROCEDURE

Experimental Alloys

The compositions of the experimental materials tested in this work are presented in Table 1. A base alloy composition of 0.3Cu-0.1C-1Mn-0.25Si was selected for this work to investigate the effects of atmospheric humidity on a Si-killed dual phase steel. A relatively high base Cu level was selected to promote Cu separation. 0.55Cu was selected for the elevated Cu condition to simulate an alloy produced from highly Cu-contaminated scrap. Each alloy was melted in a laboratory induction furnace and cast as ingots. Samples were then machined from the as-cast condition, avoiding the centerline of ingots.

Table 1 – Alloy Compositions (wt pct)

Alloy	C	Mn	**Si**	**Cu**	**Ni**	N	P	S	B
Base	0.099	1.03	**0.24**	**0.28**	**0.005**	0.0016	0.005	0.0004	0.0003
+Cu	0.099	1.01	**0.23**	**0.55**	**0.005**	0.0024	0.005	0.0004	0.0004

Thermogravimetric Analysis Procedure

A schematic depicting the TG setup used for all the isothermal oxidation experiments is shown in Figure 1(a). The TG hot-zone was a 3 cm long section of the 2 cm diameter cylindrical alumina furnace. Temperature was measured via a K-type thermocouple located within the hot-zone, directly adjacent to the sample. Gas composition was measured by mass flow controllers before entering the chamber where the N_2 and O_2 streams blend. Nitrogen gas was introduced along the column to prevent back flow of the oxidizing gases. The N2 and mixed N_2-O_2 gases were combined before entering the reaction zone to minimize convective effects. The H_2O content was measured at the chamber inlet and exit. The TG samples were 14 mm long, 4.5 mm wide, and 2.5 mm thick with a 2 mm diameter hole for fixturing, shown in Figure 1(b). Duplicate tests were conducted to verify the oxidation response. Samples were polished with 600 grit SiC paper and cleaned in acetone prior to testing.

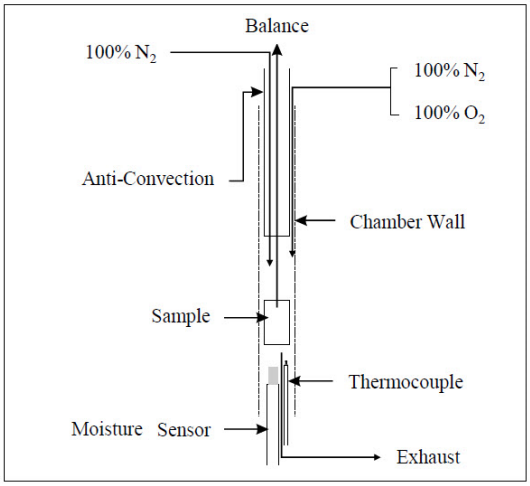

(a)

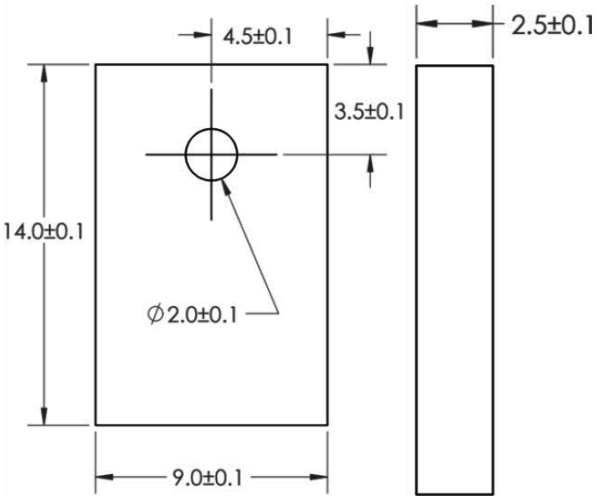

(b)

Figure 1. (a) Schematic diagram of the TGA setup used for the oxidation experiments. (b) Geometry of each sample. The nominal geometry depicted was used to calculate the initial surface area of each sample. The small hole was used to suspend the sample from the balance. Machined dimensions (mm) are indicated.

Chemically dry air was produced by blending pure N_2 and O_2 streams in an 80:20 ratio to generate the dry air atmosphere. The measured DP for this final gas blend was -28 °C, or a H_2O partial pressure of 0.46 hPa. Humidification was performed by flowing the O_2 stream through a Peltier cooler filled with heated water to humidify the O_2 stream. Initial O_2 humidification was oversaturated in H_2O to then dilute to the target DP when blended with the N_2 stream. The high humidity (wet air) condition had a DP of 35 °C or 56.5 hPa H_2O. This condition was specifically chosen to investigate ambient atmospheres during steelmaking with high H_2O content.

Samples were hung from a Pt wire connected to a separate balance to measure mass change during oxidation. Heating to 1150 °C was conducted under 100 standard cubic centimeters per minute (sccm) of N_2 and held for 10 min. Gas flow was then swapped to the oxidizing gas mixture under the same flowrate, and the sample was allowed to oxidize for 10 min. The dry and wet gas blends were flowed through separate lines during heating, stabilization, and oxidation to prevent condensation in the gas lines or oversaturation in the Peltier cooler. The total gas flow rate was kept above 4.2 $cm \cdot s^{-1}$ to prevent oxygen supply limitations during the tests[27, 28]. H_2O content and temperature were measured continuously throughout the test. The samples were cooled under a N_2 stream after each test, and the samples were removed from the chamber once fully cooled. Mass data was recorded at 10 Hz.

Microstructural Analysis

The oxidized samples were mounted in carbon-impregnated epoxy with one of the wide faces of the sample positioned as the viewing plane and examined around the sample perimeter. Samples were manually polished to a 1 μm finish, etched with 2 pct nital, and imaged via light optical microscopy (LOM) using an Olympus® DSX500. Low magnification images were taken from eight locations around the sample perimeter to measure the final external oxide thickness grown during the tests.

DISCUSSION

Oxidation Rate Data

The oxidation rates of the Base and +Cu alloys in -28 °C DP (dry) simulated air and 35 °C DP (wet) simulated air were measured using TGA at 1150 °C for 10 min. The measured mass increase over time data was normalized over the initial sample area, and the resultant oxidation data are presented in Figure 2.

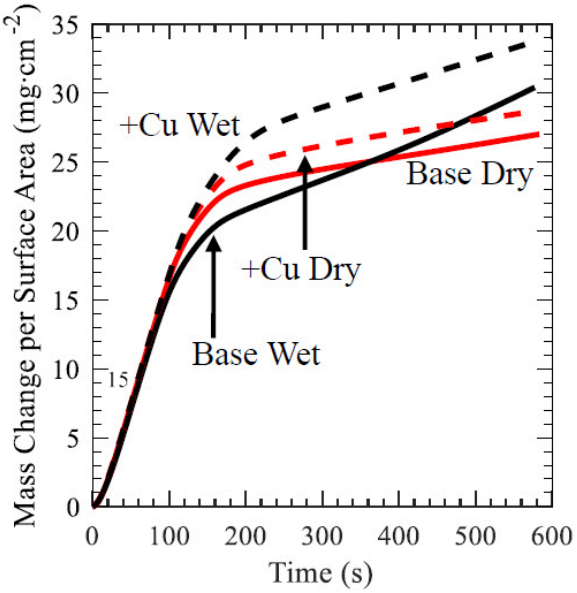

Figure 2. Mass change per surface area as a function of oxidation time for the Base and +Cu alloys oxidized at 1150 °C in simulated dry (-28 °C DP) and wet (35 °C DP) air for 10 min. Two tests were conducted to generate the average curve for each test condition.

Similar, rapid linear oxidation rates were observed for each alloy and atmosphere, confirming that O_2 supply limitations were not hampering initial oxide growth. The +Cu alloy in both atmospheres and the Base alloy in the dry atmosphere underwent the linear to parabolic transition at similar times, suggesting the latter test sample grew an oxide layer with differing diffusion

kinetics. Linear to parabolic oxidation transition is controlled by the rate-limiting kinetic step during oxidation, so a shorter linear regime suggests that the diffusion through the oxide layer became rate limiting more rapidly for the Base alloy in the wet atmosphere than the other alloy/atmosphere pairs.

The shape of the parabolic regimes was similar for both alloys in the dry atmosphere, with a low and constant growth rate that did not change throughout oxidation. Similar final masses were obtained, with the +Cu alloy growing slightly more oxide than the Base alloy. The final masses and similar linear to parabolic transition times suggest the external oxide structure was likely similar for these alloys. The final oxide scale was minimally adherent to the underlying steel for both alloys in the dry atmosphere, with significant scale spallation occurring during metallographic preparation.

Parabolic oxidation in the wet atmosphere was significantly higher for both alloys compared to the dry air condition, and a larger discrepancy between the alloys was observed. The +Cu alloy grew a larger oxide mass than the Base alloy, but had a slightly lower parabolic oxidation rate. This is due to the +Cu alloy undergoing the linear to parabolic oxidation transition at a later time such that this alloy spent more time in the linear (more rapid) growth regime. The Base alloy transitioned from linear to parabolic oxidation more rapidly than the +Cu alloy, but had a slightly higher parabolic growth rate. It is unclear why the difference in oxidation transition or parabolic growth rates were observed, as additions of Cu are not expected to dramatically impact the overall oxidation kinetics of steel[29]. The parabolic oxidation rate of the Base alloy also appeared to increase slightly during oxidation, indicating a potential change in kinetics due to the emergence of a more rapid diffusion pathway compared to the initial oxide structure at the onset of parabolic oxidation. Scale adherence after testing was notably higher than the final oxides grown on either alloy in the dry air condition, but no visual differences were observed.

Oxide Structure and Steel/Scale Interface Morphology

Dry Atmosphere

Micrographs of the steel/scale interfaces for the Base and +Cu alloy oxidized in the dry air condition are shown in Figure 3.

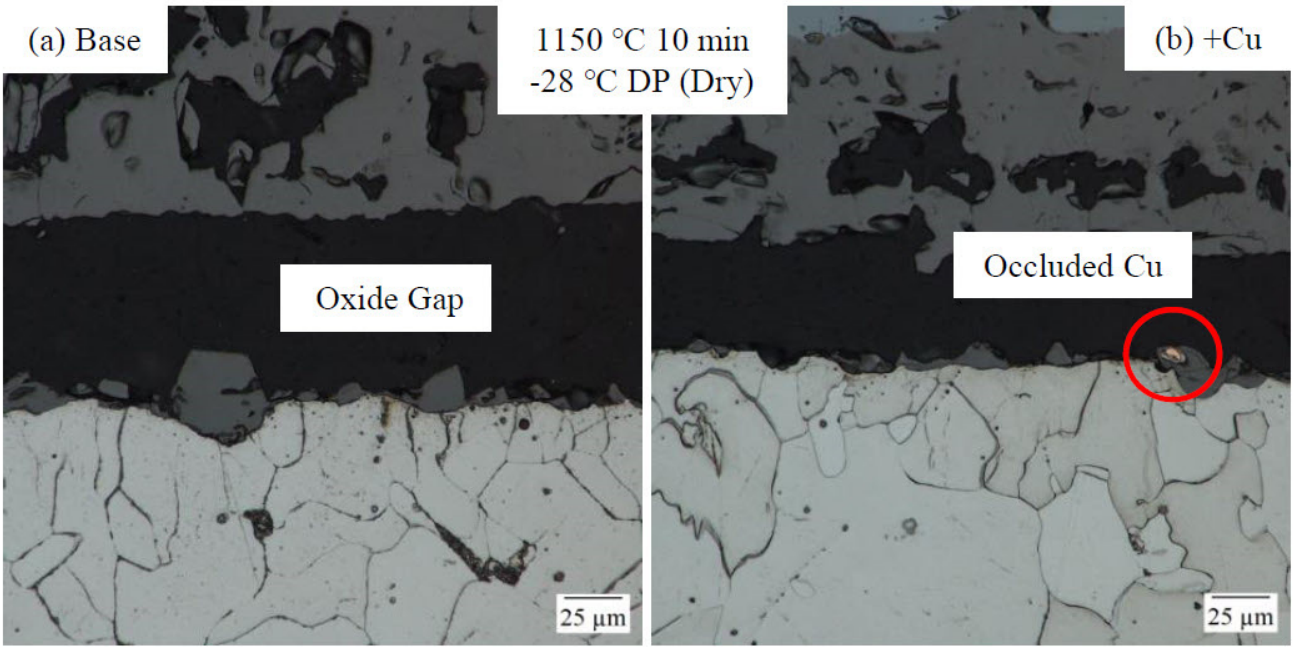

Figure 3. Representative LOM micrographs of the steel/scale interfaces for the (a) Base and (b) +Cu alloys in the dry air condition after oxidation at 1150 °C for 10 min. An oxide gap was observed continuously across the interfaces of both alloys. Cu separation was not observed in the Base alloy, but pockets of occluded Cu were observed in the +Cu along the steel/scale interface.

A porous, bilayer oxide structure was observed for both alloys. Interfacial oxide structure was similar between the Base and +Cu alloys, with minimal oxide directly attached to the base metal. A continuous steel/scale gap was found across the entire interface of each sample, noted in Figure 3(a), which may have formed during oxidation or upon cooling via unequal scale and base metal contraction. The ratio between the three Fe oxides present in the scale suggests that the gap was present for some significant time, as the ratio between FeO and Fe_3O_4 is lesser than pure Fe[30]. The presence of this gap during oxidation would decrease the parabolic oxidation rate for both alloys, which agrees with the similar and low rates observed in Figure 2.

Cu separation was observed in the +Cu alloy. Discrete particles of Cu were found along the steel/scale interface, with occluded Cu occurring where regions of oxide were in contact with the base metal underneath the steel/scale gap, as shown in Figure 3(b). Regions of Cu contact with the base metal suggest that some degree of Cu penetration and subsequent hot shortness would be possible for the +Cu alloy but not the Base alloy in the dry atmosphere. In addition to regions of dispersed Cu, some larger Cu agglomerations were observed in the +Cu alloy, shown in Figure 4. Large localized Cu buildup may be due to accelerated local oxidation or greater steel/scale contact, but no change in oxide thickness or structure were found in these regions. Increased Cu thickness may be due to a pooling phenomenon, where large Cu volumes have a tendency to pool to reduce the surface tension of the Cu liquid, without the presence of interfacial oxides to restrict Cu movement.

¶

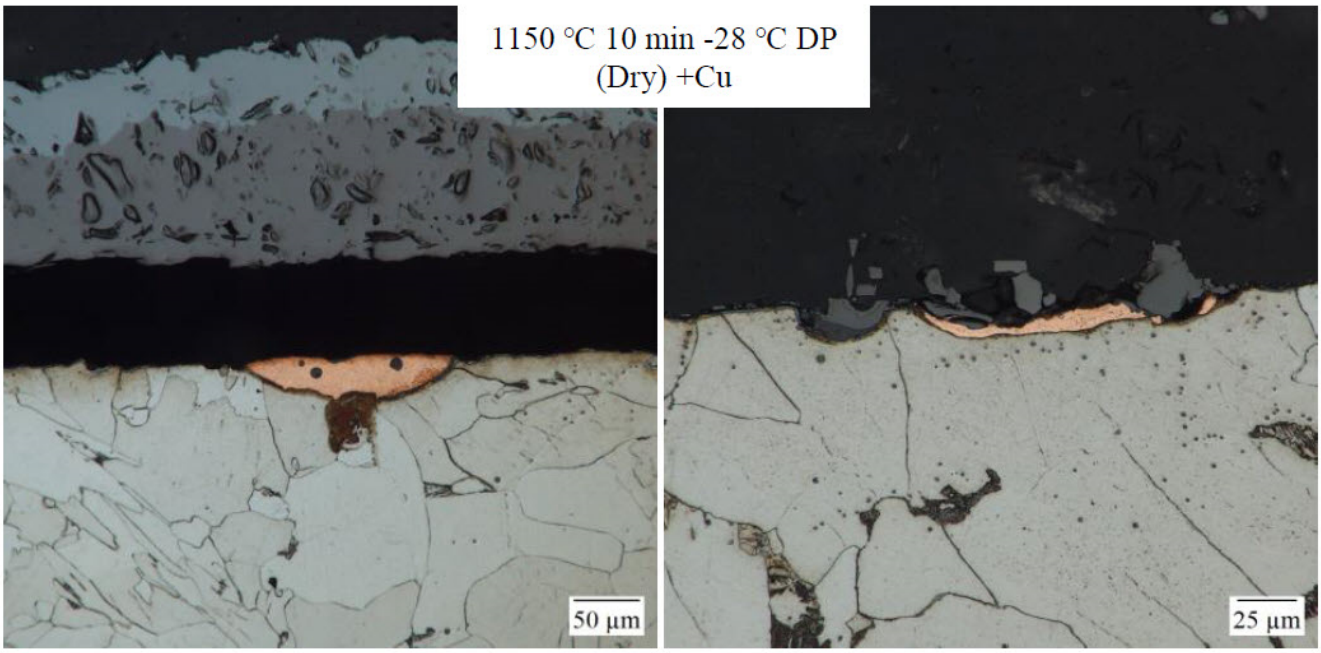

Figure 4. Local Cu buildup observed in the +Cu alloy after oxidation in the dry simulated air atmosphere. Cu pools were found in multiple locations where a gap was present during oxidation between the external scale and the steel/scale interface.

Wet Atmosphere

Micrographs of the steel/scale interfaces for the Base and +Cu alloy in the wet air oxidation condition are shown in Figure 5.

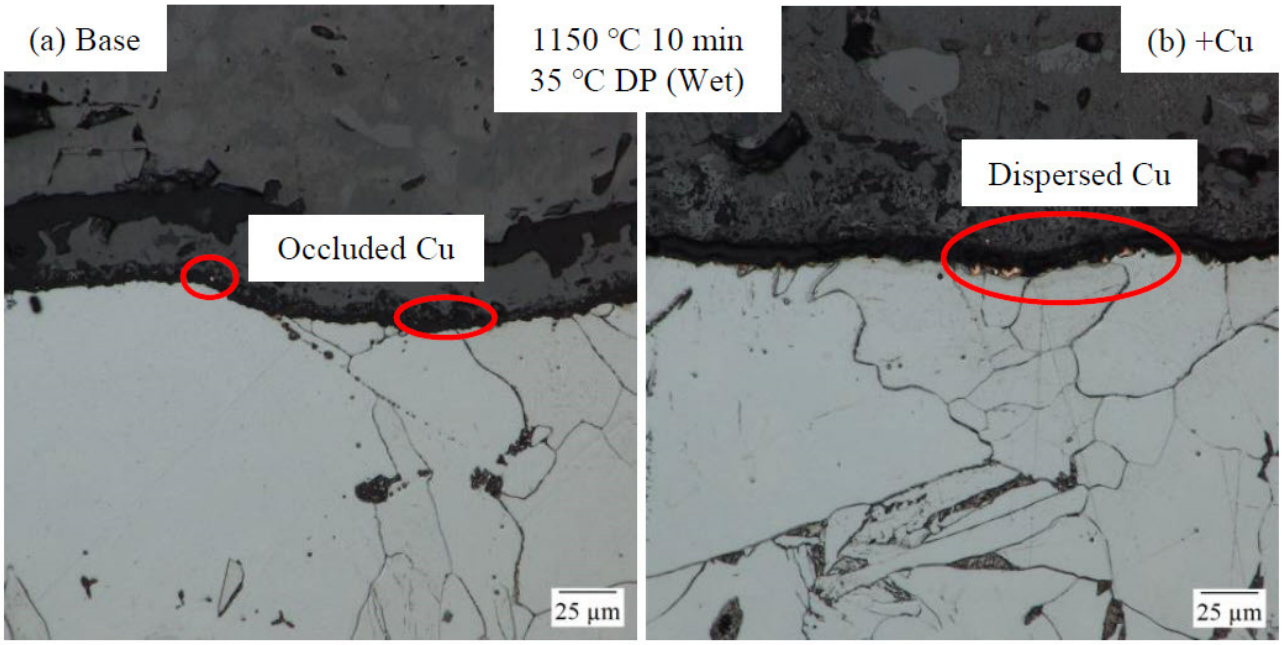

Figure 5. Representative LOM micrographs of the steel/scale interfaces for the (a) Base and (b) +Cu alloys after oxidation for 10 min at 1150 °C in the wet air condition. Good steel/scale adherence was observed across the interfaces of both alloys. Small regions of occluded Cu were found in the Base alloy, while both occluded Cu and regions of dispersed Cu along the steel/scale interface were observed in the +Cu alloy.

The external oxide structure for both alloys was significantly different in the wet air condition. Example micrographs for the Base and +Cu alloy are shown in Figure 6(a) and (b), respectively. The scale appeared porous, but with a thinner outer Fe_3O_4 layer compared to the dry atmosphere Figure 6(a)), a large middle FeO layer, and a region of oxide not present in the dry air condition. This local oxide appeared to increase steel/scale adherence along regions of the surface where it was present, as seen in Figure 6(a). The feature length and structure suggest this region is composed of one or more oxide phases not present in the dry air condition. Based upon the alloy composition, these fine-scale oxides are Si-rich, confirmed by EDS point scan analysis, and likely contribute to the change in oxidation kinetics observed for the wet air condition. This oxide is likely fayalite, Fe_2SiO_4. The continuous gap observed in the dry air condition was no longer found. A discontinuous interface gap was present, visible in Figure 6(b), with less interfacial oxide present in these regions.

Cu separation was observed in both alloys in the wet air condition. Cu separation behavior was observed as occluded Cu in the Base alloy, Figure 5(a), and as finely dispersed along the steel/scale interface in the +Cu alloy, Figure 5(b). More Cu phase was present in the +Cu alloy compared to the Base alloy. No regions of large Cu pooling or agglomeration were observed. This difference in Cu distribution compared to the dry air condition is likely due to the large difference in interfacial oxide morphology between the atmospheres. Good steel/scale adherence and the presence of a finer-scale interface oxide correlated strongly with the presence of finely dispersed or occluded Cu in this condition. Finely dispersed Cu was not observed in the dry air test condition, which did not exhibit steel/scale interface adherence.

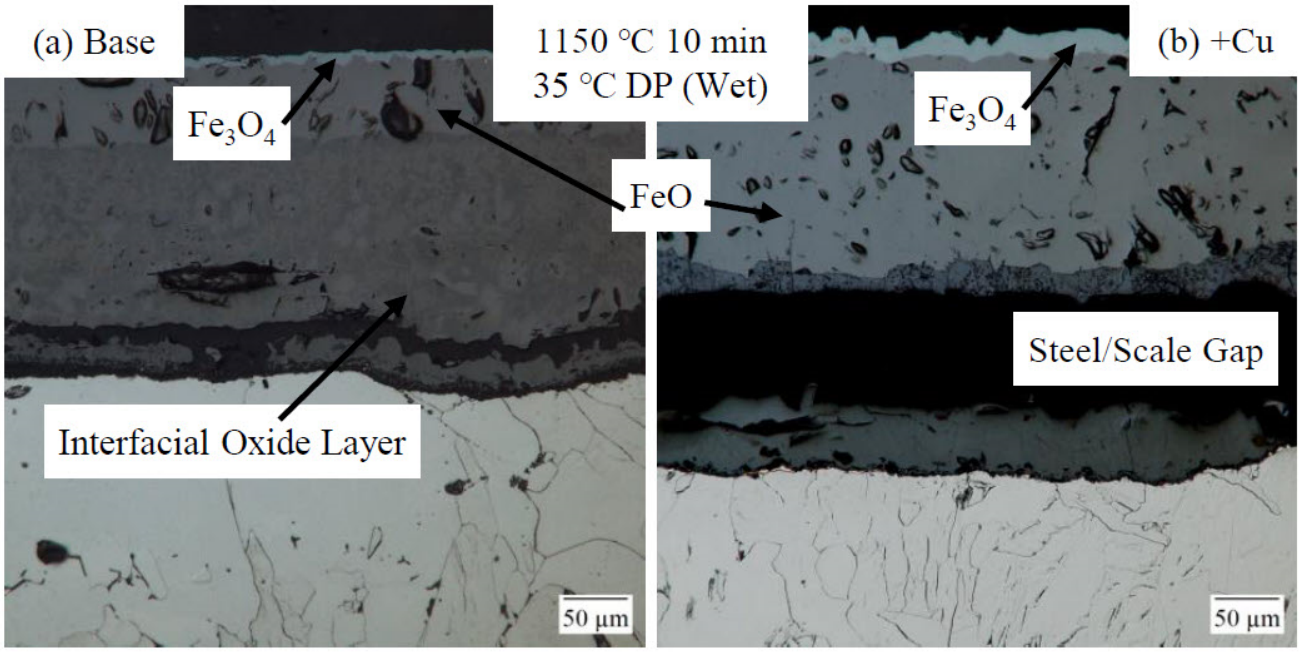

Figure 6. External oxide structure for the (a) Base and (b) +Cu alloys after oxidation for 10 min at 1150 °C in the wet simulated air condition. Regions with good steel/scale adherence exhibited the large interfacial structure shown in (a), while regions with a steel/scale gap resembled the structure shown in (b).

External Oxide Thickness Measurements

Final oxide thickness measurements for the Base and +Cu alloys from both atmospheres are shown in Figure 7. Measurements were taken from four locations in each of eight micrographs around the surface perimeter alloy and test condition.

Both alloys exhibited comparable final oxide thickness to each other for a given oxidizing atmosphere. The Base alloy grew a slightly thicker oxide in the dry atmosphere while the +Cu alloy grew a slightly thicker oxide in the wet atmosphere, but the alloy composition did not appear to significantly contribute to changes in oxide growth for a given oxidation condition. The similar final oxide thickness is surprising for the wet atmosphere considering the relatively different parabolic oxidation rate and final mass gain observed in the wet air condition, Figure 2.

Larger variability in final oxide thickness measurements were found for the wet air condition for both alloys, suggesting the higher DP contributed to a more inconsistent oxide final structure compared to the lower DP condition. This is likely due to gap formation between the external scale and the steel/scale interface, either during oxidation or during cooling of the dry air samples. The absence of this gap and the presence of the fine-scale, likely Si-rich oxide in the wet atmosphere are probably large contributors to the dramatic increase in final oxide thickness. The significantly thicker final oxide for the wet air condition suggests greater Cu supply to the steel/scale interface during oxidation, as more base metal has been transformed to oxide to form this thicker layer.

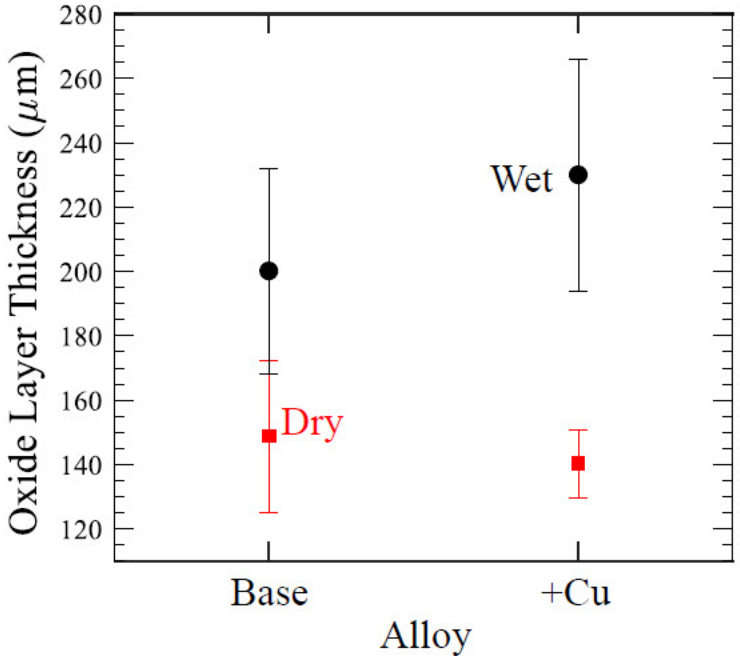

Figure 7. Oxide thickness measurements for the Base and +Cu alloys after oxidation in dry (-28 °C DP) and wet (35 °C DP) air for 10 min at 1150 °C. A significant increase in oxide thickness for both alloys was found with increasing atmospheric humidity.

CONCLUSIONS

Alloys containing appreciable Si and Cu undergo a dramatic change in oxidation behavior when exposed to 35 °C DP air compared to -28 °C DP air at 1150 °C for 10 min. The parabolic oxidation rate increases substantially and there is a change in the linear to parabolic oxidation transition. Additions of 0.25 wt pct Cu to an alloy containing 0.3Cu-0.25Si did not impact the oxidation behavior in -28 °C DP air, but did alter the behavior in 35 °C DP air. Cu separation was observed in alloys in the 35 °C DP air, while the Base alloy did not separate Cu in the -28 °C DP air conditions. Increasing DP promoted the formation of a fine-scale Si-rich interfacial oxide, likely fayalite, which contributed to the separated Cu collected as dispersed particles along the interface rather than large pools. The 35 °C DP air tests grew thicker oxides than the -28 °C DP air tests, suggesting the higher DP promotes a greater supply of Cu to the steel/scale interface. Increasing Cu supply contributes to greater liquid Cu volume available to penetrate along the austenite grain boundaries. The wet atmosphere promoting greater occlusion for the same alloy composition suggests that wetter atmospheres may require lesser alloy additions to promote the same degree of occlusion, and drier oxidation conditions may necessitate greater alloying to offset the formation of Cu hot shortness due to Cu pooling at the steel/scale interface.

ACKNOWLEDGEMENTS

The authors gratefully acknowledge the support of the industrial sponsors of the Advanced Steel Processing & Products Research Center (ASPPRC) at the Colorado School of Mines in Golden, CO. This work was also supported by the Department of Energy's Advanced Manufacturing Office under Grant No. DE-EE0009389

REFERENCES

1. W. Salter, “Effects of Alloying Elements on Solubility and Surface Energy of Copper in Mild Steel,” Journal of the Iron and Steel Institute, vol. 204, 1966, pp. 478–488.
2. D.A. Melford, “The Influence of Residual and Trace Elements on Hot Shortness and High Temperature Embrittlement,” Philosophical Transactions of the Royal Society of London., vol. 295, no. 1413, 1980, pp. 89–103.
3. L. Habraken and J. Lecomte-Beckers, “Hot Shortness and Scaling of Copper Containing Steels,” in Copper in Iron and Steel, Wiley & Sons, 1982, pp. 45–81.
4. A. Nicholson and J.D. Murray, “Surface Hot Shortness in Low-Carbon Steel,” Journal of the Iron and Steel Institute, vol. 203, no. 10, 1965, pp. 1007–1018.
5. V. Leroy, “Effects of Tramp Elements in Flat and Long Products,” Office for Official Publications of the European Communities, Luxembourg, Technical Steel Research No. EUR 16672, Mechanical Working, 1995.
6. D. Coutsouradis, V. Leroy, T. Greday, and J. Lecomte-Beckers, “Review of Hot Shortness Problems in Copper- Containing Steel,” ATB Métallurgie, vol. 23, no. 3, 1983, pp. 1–24.
7. J. Oda, K. Akimoto, and T. Tomoda, “Long-Term Global Availability of Steel Scrap,” Resources, Conservation and Recycling, vol. 81, 2013, pp. 81–91.
8. D. Janke, L. Savov, H. Weddige, and E. Schulz, “Scrap-Based Steel Production and Recycling of Steel,” Materiali in Tehnologije, vol. 34, 2000, pp. 387–399.
9. O. Rod, C. Becker, and M. Nylén, “Opportunities and Dangers of Using Residual Elements in Steels: A Literature Survey,” Jernkontoret, Stockholm, Sweden, Literature Survey No. IM-2006–124, 2006.
10. K. Noro, M. Takeuchi, and Y. Mizukami, “Necessity of Scrap Reclamation Technologies and Present Conditions of Technical Development,” ISIJ international, vol. 37, no. 3, 1997, pp. 198–206.
11. J. Kim, B.K. Sovacool, M. Bazilian, S. Griffiths, J. Lee, M. Yang, and J. Lee, “Decarbonizing the Iron and Steel Industry: A Systematic Review of Sociotechnical Systems, Technological Innovations, and Policy Options,” Energy Research & Social Science, vol. 89, 2022, pp. 1–32.
12. D. Raabe, M. Jovičević-Klug, D. Ponge, A. Gramlich, A. Kwiatkowski Da Silva, A.N. Grundy, H. Springer, I. Souza Filho, and Y. Ma, “Circular Steel for Fast Decarbonization: Thermodynamics, Kinetics, and Microstructure Behind Upcycling Scrap into High-Performance Sheet Steel,” Annual Review of Materials Research, vol. 54, no. 1, 2024, pp. 247–297.
13. K.E. Daehn, A. Cabrera Serrenho, and J.M. Allwood, “How Will Copper Contamination Constrain Future Global Steel Recycling?,” Environmental Science & Technology, vol. 51, no. 11, 2017, pp. 6599–6606.
14. E.T. Turkdogan, W.M. McKewan, and L. Zwell, “Rate of Oxidation of Iron to Wustite in Water-Hydrogen Gas Mixtures,” The Journal of Physical Chemistry, vol. 69, no. 1, 1965, pp. 327–334.
15. H. Selenz and F. Oeters, “A Contribution to the Scaling of Steel in Technical Flue Gases,” Archiv für das Eisenhüttenwesen, vol. 55, no. 5, 1984, pp. 201–208.
16. F.S. Pettit and J.B. Wagner, “Transition from the Linear to the Parabolic Rate Law During the Oxidation of Iron to Wüstite in CO-CO2 Mixtures,” Acta Metallurgica, vol. 12, no. 1, 1964, pp. 35–40.
17. H.T. Abuluwefa, R.I.L. Guthrie, and F. Ajersch, “Oxidation of Low Carbon Steel in Multicomponent Gases: Part I. Reaction Mechanisms during Isothermal Oxidation,” Metallurgical and Materials Transactions A, vol. 28, no. 8, 1997, pp. 1633–1641.
18. ¶H.T. Abuluwefa, R.I.L. Guthrie, and F. Ajersch, “Oxidation of Low Carbon Steel in Multicomponent Gases: Part II. Reaction Mechanisms During Reheating,” Metallurgical and Materials Transactions A, vol. 28, no. 8, 1997, pp. 1643– 1651.
19. K. Sachs and C.W. Tuck, “Scale Growth during Re-heating Cycles,” Materials and Corrosion, vol. 21, no. 11, 1970, pp. 945–954.
20. C.W. Tuck, M. Odgers, and K. Sachs, “Scaling Rates of Pure Iron and Mild Steel in Oxygen, Steam, Carbon Dioxide in the Range 850-1000C,” Anti-Corrosion Methods and Materials, vol. 13, no. 7, 1966, pp. 17–21.
21. C.W. Tuck, M. Odgers, and K. Sachs, “The Oxidation of Iron at 950°C in Oxygen/Water Vapour Mixtures,” Corrosion Science, vol. 9, no. 4, 1969, pp. 271–285.
22. D.B. Lee and J.W. Choi, “High Temperature Oxidation of Steels in Air and CO2–O2 Atmosphere,” Oxidation of Metals, vol. 64, no. 5, 2005, pp. 319–329.

23. H.J. Grabke, V. Leroy, and H. Viefhaus, “Segregation on the Surface of Steels in Heat Treatment and Oxidation,” ISIJ International, vol. 35, no. 2, 1995, pp. 95–113.

24. S.W. Kim and H.G. Lee, “Effect of Oxide Scale Formation on the Behaviour of Cu in Steel during High Temperature Oxidation in O2-N2 and H2O-N2 Atmospheres,” Steel Research International, vol. 80, no. 2, 2009, pp. 121–129.

25. K. Shibata, S.J. Seo, M. Kaga, H. Uchino, A. Sasanuma, K. Asakura, and C. Nagasaki, “Suppression of Surface Hot Shortness Due to Cu in Recycled Steels,” Materials Transactions, vol. 43, no. 3, 2002, pp. 292–300.

26. R.Y. Chen and W.Y.D. Yuen, “Copper Enrichment Behaviours of Copper-Containing Steels In Simulated Thin-Slab Casting Processes,” ISIJ International, vol. 45, no. 6, 2005, pp. 807–816.

27. H. Abuluwefa, R.I.L. Guthrie, and F. Ajerscht, “The Effect of Oxygen Concentration on the Oxidation of Low-Carbon Steel in the Temperature Range 1000 to 1250 C,” Oxidation of Metals, vol. 46, 1996, pp. 423–440.

28. Y.R. Chen, “Oversight or New Insight? Comments on Several Recent Papers Studying High-Temperature Oxidation of Si-Containing Steels,” Oxidation of Metals, vol. 93, no. 1–2, 2020, pp. 1–15.

29. B. Webler, L. Yin, and S. Seetharaman, “Effects of Small Additions of Copper and Copper + Nickel on the Oxidation Behavior of Iron,” Metallurgical and Materials Transactions B, vol. 39, no. 5, 2008, pp. 725–737.

30. J. Païdassi, “The Kinetics of the Air Oxidation of Iron in the Range 700–1250°C,” Acta Metallurgica, vol. 6, no. 3, 1958, pp. 184–194.

